# Development and application of a new tool for lithographic mask evaluation, the stepper equivalent Aerial Image Measurement System, AIMS

by R. A. Budd
D. B. Dove
J. L. Staples
R. M. Martino
R. A. Ferguson
J. T. Weed

**This paper describes the development of a new tool for evaluating lithographic masks, its software, and its application to the development of advanced mask designs, including phase-shifted features. This mask-imaging system, known as the stepper equivalent Aerial Image Measurement System (AIMS™), provides a means for rapid evaluation of masks. The key feature of AIMS is that the mask is imaged under conditions that emulate the image produced by a given lithographic exposure tool onto a resist layer. In the AIMS microscope, the image obtained is enlarged so as to permit quantitative measurement with a low-noise CCD camera. A quantitative record of selected features of the mask is useful in predicting the printability window for given mask and stepper combinations. Details of the optical system and extensive software capability are given, and examples are presented of feature printability of phase-shifted features, optical proximity, and other effects. Applications include the prediction of key critical mask dimensions as a function of exposure and depth of focus and the rapid checking of the**



**0018-8646/97/$5.00 © 1997 IBM**

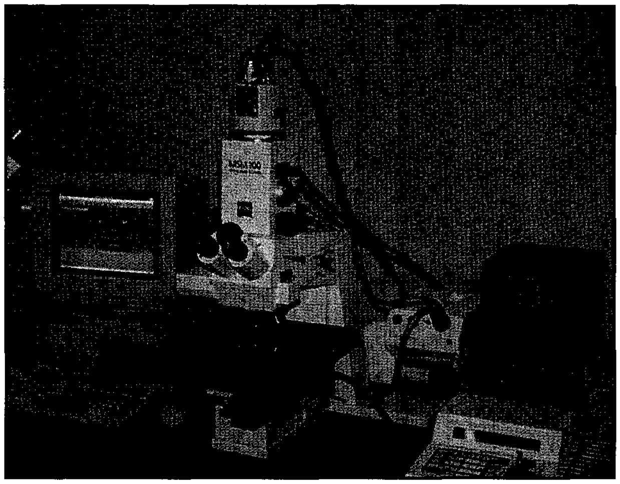

**Figure 1**

Photograph of the Microlithography Simulation Microscope, MSM100. (Reprinted courtesy of Carl Zeiss Inc.)

**effectiveness of repair actions prior to validation by resist runs. The AIMS microscope system is available as the Carl Zeiss MSM100 Microlithography Simulation Microscope and is now in use in a number of companies as a new tool for mask fabrication and development.**

## Introduction

The continuing drive to extend the capability of optical lithography to increasingly smaller dimensions has led to the development of exposure tools of higher numerical aperture (NA) and shorter wavelengths, to the exploration of new mask technologies such as phase-shift methods [1, 2], and to the refinement of mask layouts to include optical proximity effects.

Mask design has become increasingly complex, since it is difficult to predict the printing characteristics of a mask exposure tool combination solely from knowledge of the layout geometry. Extensive use of computer programs such as Splat or Image is commonly the primary means for understanding the through-focus behavior for mask features such as parallel lines with phase shift or vias with attenuating phase shift. After mask design and fabrication, the printing characteristics of the mask are studied by printing a matrix covering a range of exposures and focus settings. These experimental test chips are then parted, and key features are measured using a scanning electron microscope; this is a time-consuming procedure.

The Aerial Image Measurement System (AIMS™)[1] was designed to provide a means for rapidly evaluating the exposure and depth-of-focus characteristics of real masks, including chrome, proximity-corrected, phase-shifted, or attenuating phase types, prior to resist validation. This device has been found to provide a new means for examining masks capable of providing useful information in a very short time before resist experiments are undertaken [3–5].

A UV microscope was set up in which the NA of the imaging lens was adjusted so that the image produced possesses the same resolution characteristics as that of a particular stepper. In order to emulate effects introduced by phase shifts or optical proximity, the masks are imaged at the wavelength of use (in the present case, 365 or 248 nm). An aperture was also placed in the illumination system so that coherence could be matched and explored. In addition, multiple off-axis apertures may be used to emulate off-axis illumination such as the Canon or Nikon approach. Initial experiments were carried out in which images were compared with extensive computer simulation and with resist features for a wide variety of cases. Good agreement was found between computer simulations and AIMS images obtained for test masks under a variety of conditions. In most cases it is sufficient to predict resist behavior via a high-contrast resist model. If desired, the image data may be used as a starting point for more extensive resist calculations.

## Tool development and description

Early in the development of phase-shift masks at IBM, it became clear that a method of evaluating photomask performance more rapidly than time-consuming traditional means was urgently needed. A novel laboratory setup consisting of an industrial microscope modified to control illumination $\sigma$ and objective lens NA was developed to emulate the imaging characteristics of an optical stepper. From the prototype, a commercial version was co-developed with Carl Zeiss Inc. and is available as the Microlithography Simulation Microscope, MSM100 (**Figure 1**). **Figure 2** shows a schematic layout of the MSM100 tool, which is based upon a deep-UV Axiotron microscope with several important differences that allow it to emulate optical steppers. Illumination is provided by a 100-W mercury arc lamp for I-line and deep-UV (365- and 248-nm) imaging, and by a halogen lamp for visual inspection and alignment. Light from the mercury lamp is prefiltered by a cold mirror, dumping excess IR radiation into a heat sink. A narrow-bandpass filter, mounted in an automatic filter changer, establishes the center wavelength (either 365 or 248 nm) with a bandwidth of typically <10 nm FWHM. The coherence or $\sigma$ of the light incident upon the photomask is controlled by an aperture positioned at a point in the base of the microscope conjugate with the objective lens pupil. This $\sigma$ aperture is mounted on a slider so that various sizes may be easily

[1] Patent applied for in 1994.

selected. New optical steppers from Canon or Nikon incorporate off-axis illumination sources to improve the resolution of the stepper. These illumination sources can also be studied with the AIMS microscope by inserting the appropriately shaped aperture into the $\sigma$ slider. The condenser lens focuses the illumination onto a small (submillimeter) region of the photomask. This focusing differs from that of the optical stepper, in which a large area of the mask is illuminated. Five- or six-inch photomasks may be mounted on the 8 × 8-in. motorized stage. The stage is driven vertically to collect through-focus image data. One feature of the optical system is that a large focus motion of the microscope stage corresponds to a small amount of defocus within a lithographic exposure tool; thus, defocus conditions of only a fraction of a micron may be readily simulated. The imaging system NA is controlled by an aperture mounted on a slider in the upper column of the microscope. A two-stage optical system magnifies the mask image onto a Photometrics high-sensitivity UV CCD camera, which is liquid-cooled to −40°C to ensure low noise. The 1317 × 1035-pixel-array camera has an intensity resolution of 12 bits per pixel, sufficient for quantitative image data analysis. The performance of the AIMS microscope was verified for a series of $\sigma$s and NAs by comparing image data with computer simulations and resist features; good correlation was shown [3].

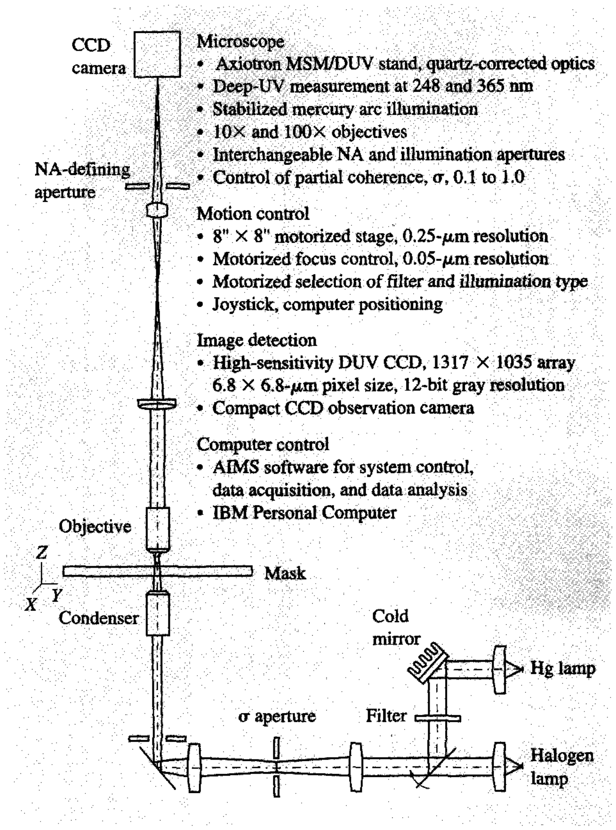


**Figure 2**

Layout and system description of the MSM100. (Reprinted courtesy of Carl Zeiss Inc.)

- *Software package*

An extensive software package was developed to provide a user-friendly graphical interface for the AIMS setup, control, data collection, and analysis. The program was written in Microsoft Visual C++™ for the Microsoft Windows® operating system. The C++ class structure provides a modular environment for easy program extendibility.

The program software communicates with the AIMS tool through a serial communication port to the Zeiss MCU26 microscope stage, as well as through a custom ISA bus adapter to the Photometrics camera. The serial link controls the stage position, filter changer, and lamp selector. The AIMS program, communicating with the Photometrics camera adapter, quickly transfers image data from the camera to the computer memory.

The program provides easy management of a variety of tool control functions. The camera type, speed, and resolution, the MCU26 controller parameters, and the objective lens calibration file are initialized on start-up of the program to their last saved values. All of these parameters can be changed through program menus. An interactive graphical display shows the current position of the lamp selector, the filter changer, the lens turret, and the dark- and bright-field sliders. Additional routines provide for aperture alignment, mask focus, and mask positioning.

After loading a mask onto the stage, it is often desirable to determine the correlation between mask and stage coordinates. By using common alignment marks on the mask and following a three-point alignment process, mask rotation and magnification correction factors are determined. This permits quick and accurate mask positioning to desired mask or stage coordinates. A KLA inspection machine is commonly used to check a mask for defects. This inspection results in a report or list of potential defect sites. The list is easily imported into the AIMS program and used to move the mask swiftly from site to site to evaluate the printability of these defects.

To assist the data acquisition process, several image-capture parameters and routines are available: a quick image preview and alignment mode, image size, and exposure settings. Since features on a photomask are usually 1–3 μm in size (for 5× masks), it is not necessary to capture and store the entire 100 × 128-μm region of the mask that is optically imaged onto the camera. A subfield is often specified defining the region of interest. Once set

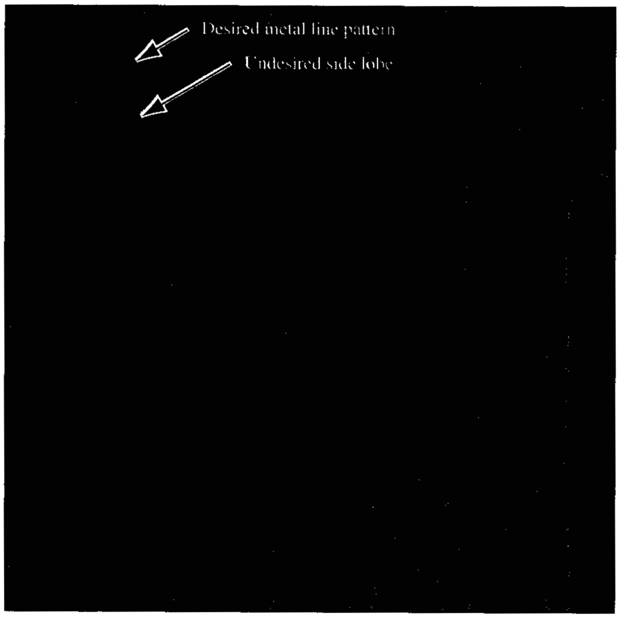


**Figure 3**

Captured aerial image of an experimental DRAM metal line layer.

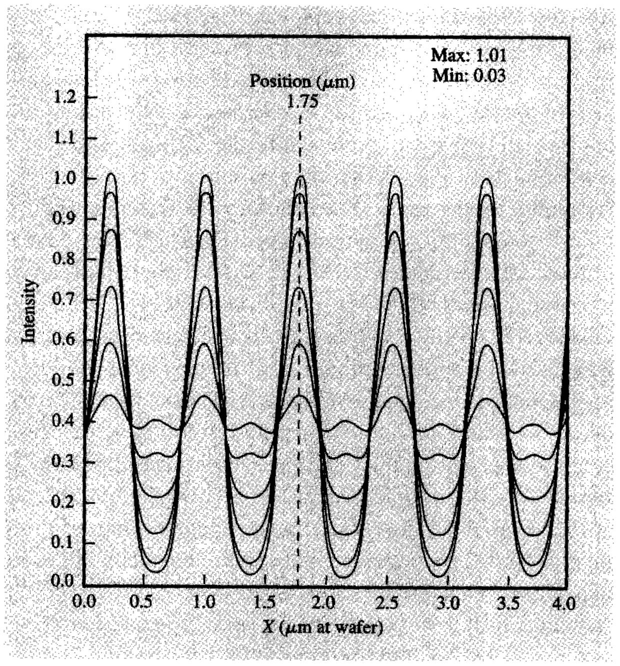


**Figure 5**

Plot of intensity profiles vs. position for a 0.35-$\mu$m line/space pattern.

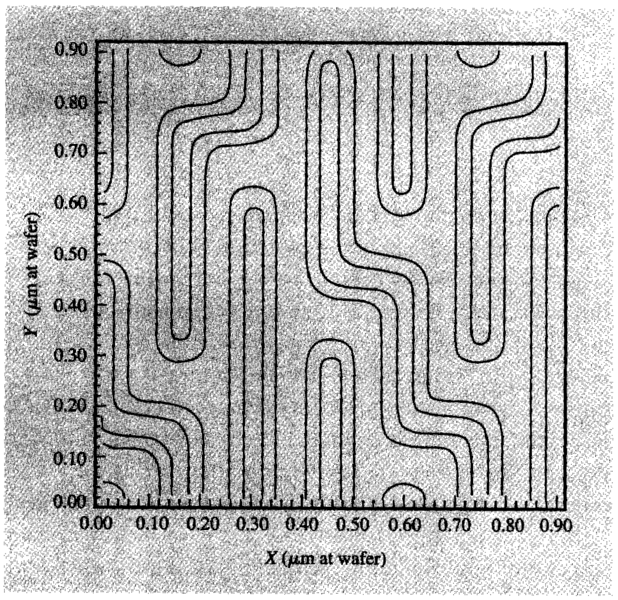


**Figure 4**

Contour plot analysis of the metal line layer shown in Figure 3. By choosing an appropriate resist exposure threshold, the desired metal line pattern may be optimized, and the undesirable side lobes that appear in Figure 3 are not printed.

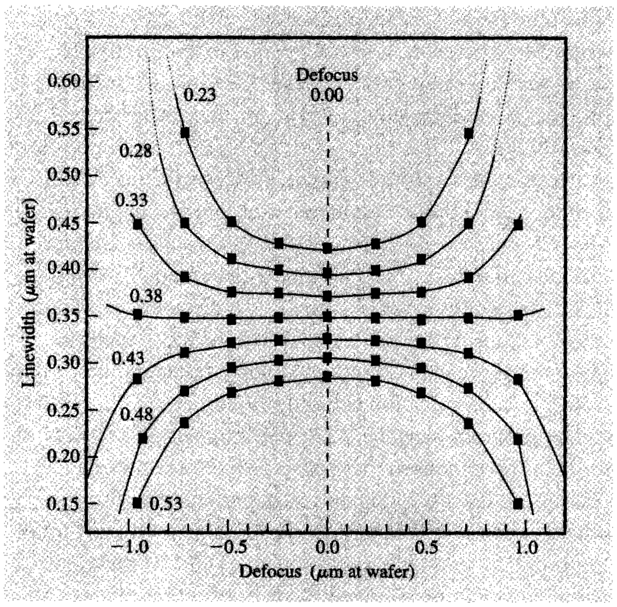


**Figure 6**

Plot of linewidth vs. defocus for a 0.35-$\mu$m line/space pattern.

up, single-focus images and/or through-focus images may be acquired and stored for further analysis. For documentation purposes, a data header is attached to each image file to record the mask designation, measurement conditions, and user comments.

• *Image analysis*

A variety of image analysis and data display routines are built into the AIMS software program. Upon capture, the image is displayed on the screen using either a linear gray-scale, pseudo-color, or threshold-highlight palette, thus providing a qualitative picture of the data (**Figure 3**). A contour plot may then be calculated for a series of intensity threshold values (**Figure 4**). The contour plot provides a quick approximation of how the image would print in a high-contrast resist at specified threshold values.

To provide quantitative views of the data, plots showing profile, linewidth versus threshold, linewidth versus defocus, and exposure defocus are available. Profile plots (**Figure 5**) may be calculated for a vertical or horizontal slice of the image. The mouse may be used to select a single bright or dark feature in the profile plot for further analysis. The linewidth versus defocus plot (**Figure 6**) is determined by calculating the width of the selected feature for specified intensity thresholds over the range of focus. This analysis method provides a quick means of determining expected resist feature linewidth variations versus defocus. Finally, the exposure defocus plot (**Figure 7**) is calculated by further specifying the permitted tolerance in feature size and plotting the limits in exposure over the range of focus.

These analysis methods are extremely valuable in determining the printability of mask defects. While conventional mask inspection tools may determine defect size, other factors (such as edge wall shape and defect phase) are not easily measured. The AIMS tool measures the aerial imaging performance of the mask directly, combining effects of mask amplitude, phase, and surface topography, a result not obtained by other inspection methods. Further analysis of the image may be performed by importing the data file into an advanced workstation program, for example to perform photoresist development simulations.

Photolithography involves many factors such as the reticle, exposure system, and photoresist process which influence the final result obtained on the substrate. These factors typically have a complex relationship to the final results and require numerous experiments for optimization. The typical time required to perform an experiment capable of assessing the performance of a lithography system can range from several days to several months, depending on the complexity of the experiment. The AIMS technology of rapid measurement and image analysis offers a means of emulating the lithography system by significantly reducing the time and cost required to evaluate lithographic performance.

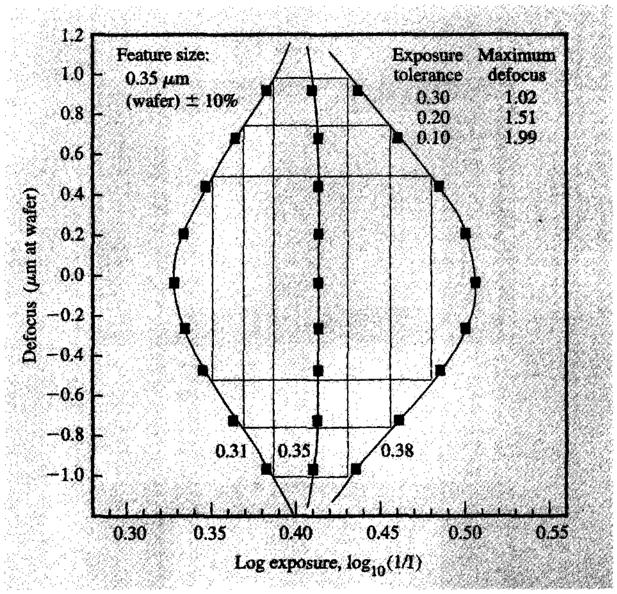


**Figure 7**

Analysis of exposure vs. defocus for a 0.35-μm line/space pattern.

## Applications of AIMS

While each component of the lithography system is important to the overall performance, the mask or reticle technology is rapidly becoming a critical and complex element of the process. The masks/reticles are either binary intensity masks (BIMs), in which the circuit pattern is defined on a quartz substrate by an opaque material (Cr/CrO), or phase-shift masks (PSMs), in which mask materials and/or topography are utilized to delineate phase-shifted regions which modify the wavefronts incident on the wafer through destructive interference. This modification can result in improved resolution, exposure latitude, and/or depth of focus relative to BIMs. Unfortunately, improved performance is obtained at the expense of increased complexity in the reticle fabrication process. In addition to transmission, phase must also be controlled.

While a variety of PSM techniques exist (attenuated, alternating, rim, and outrigger), the attenuated and alternating techniques are the most generally studied. In the attenuated PSM, the dark areas of the mask typically transmit the exposure energy (5–10% relative intensity) with a 180° phase relative to the clear areas [6]. The alternating PSM method of Levenson et al. [1] utilizes alternating light regions to transmit exposure energy (100% relative intensity) with a 180° phase relative to a neighboring

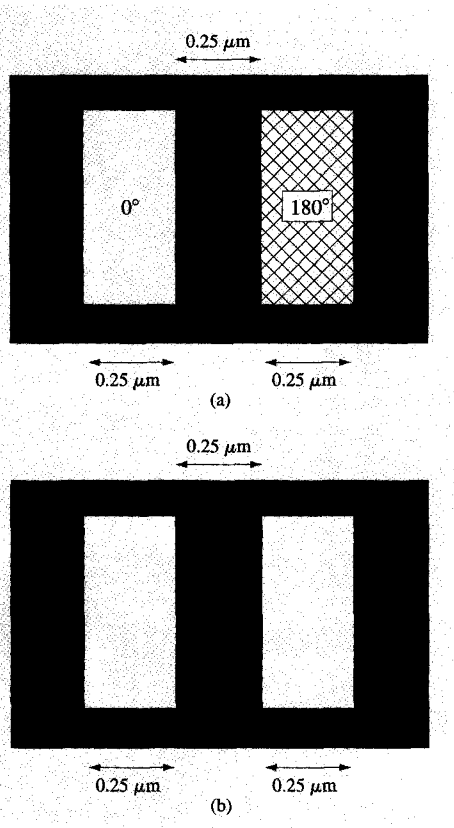


**Figure 8**

(a) Alternating phase and (b) binary PSM designs for a special feature within a 0.25-μm DRAM cell. (Reprinted with permission from [5]).

light region [7]. Additive or removal techniques may be used to create alternating phase structure (among which etched quartz technology is the most prevalent).

Inaccurate control of fabrication parameters for a PSM can have a detrimental impact on lithographic performance. There may be deviations from theory, such as transmission reduction through a phase-shifted opening which is dependent on etch roughness as well as electromagnetic scattering phenomena from the sidewalls of the etched opening. In addition to transmission, phase errors will exist if the correct material depth relative to the refractive index is not obtained. This error may be produced by etch endpoint inaccuracy during quartz removal in a subtractive quartz process, and film property imperfections may be produced by variations in an attenuated film deposition process.

Fabrication processes have been developed to address these deviations from theory in order to optimize lithographic performance. A post-etch treatment (also referred to as an etch-back process), in which an isotropic wet etch moves the etched-quartz sidewalls beneath the bordering chrome film, compensates for the strong impact of electromagnetic scattering [8]. AIMS measurements were used to fine-tune this process on a special feature in a 0.25-μm DRAM cell design [5], as shown in **Figure 8**. The aerial image measurement in **Figure 9** demonstrates the effect of the etch-back process on the amount of optical scattering in the phase-shifted opening. The optical scattering produces an intensity transmission error, as seen on the no-etch case, by its reduced peak intensity. The peak intensity of the phase-shifted opening clearly increased relative to the non-phase-shifted opening as the wet-etch depth increased. Optimum lithographic performance was identified with an approximate etch-back of 1200 Å [5].

Phase optimization for alternating and attenuated PSM processes was also established by applying the AIMS.

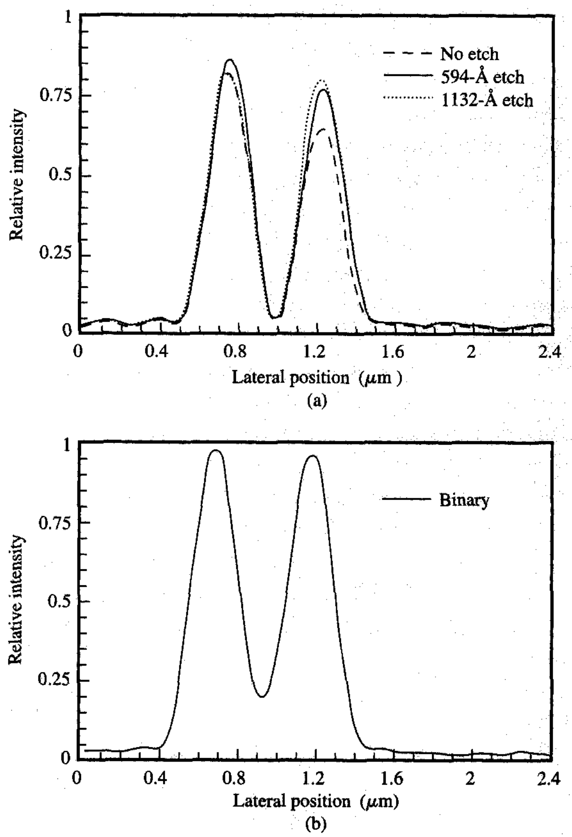


**Figure 9**

AIMS measurements of the intensity distribution for the 0.25-μm features of DRAM patterns with various post-etch treatments shown in Figure 8: (a) alternating phase; (b) binary. (Reprinted with permission from [5]).

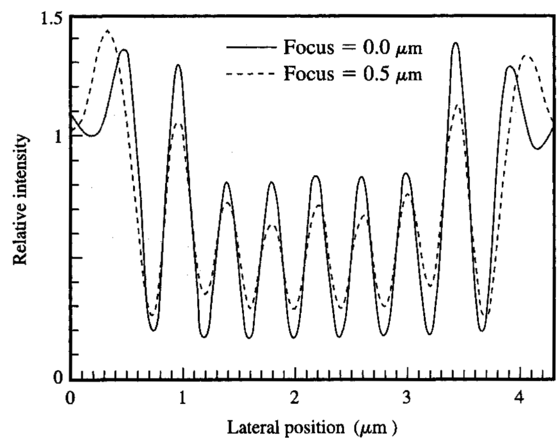


**Figure 10**

AIMS measurements of a 0.2-$\mu$m alternating line/space pattern.

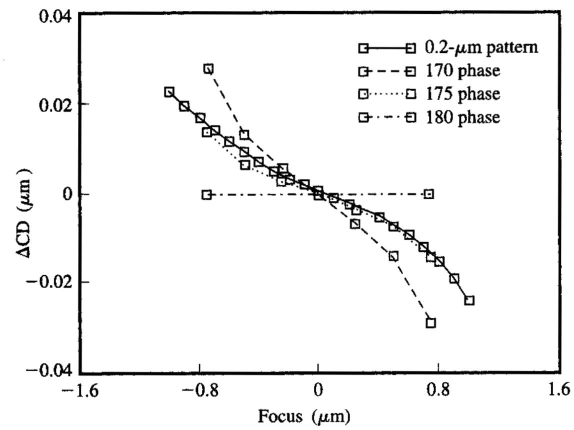


**Figure 11**

Plot of difference in critical dimension (CD) vs. focus at multiple thresholds for the 0.2-$\mu$m line/space data of Figure 10.

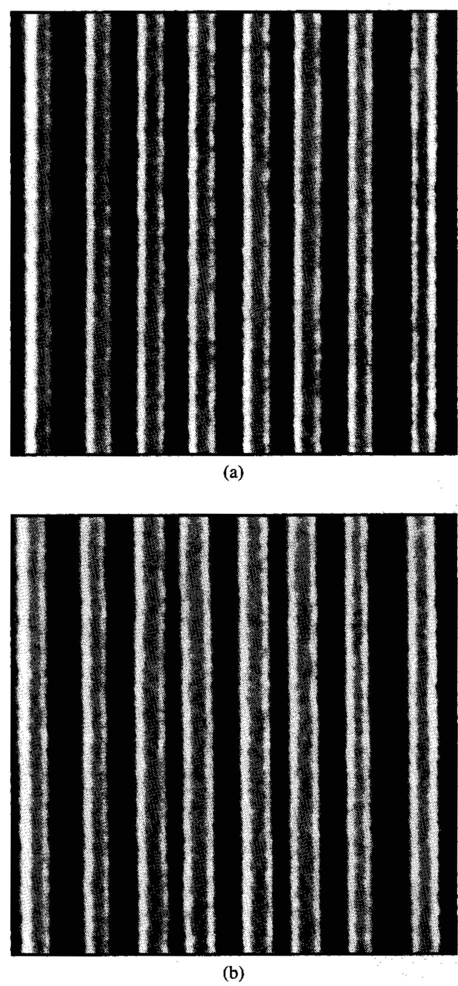


**Figure 12**

SEM photos of 0.2-$\mu$m line/space features printed in APEX-E (0.61-$\mu$m) resist on an SVGL Micrascan II stepper at 0.3$\sigma$: (a) in focus; (b) defocused.

Alternating PSM processes have an inherent asymmetry when the phase is not ideal. This asymmetry provides a method of extraction which relies on a comparison of the size of adjacent features through focus. This difference in size of adjacent openings of opposite phase ($\Delta$CD) can be expressed in terms of a phase error,

$$\Delta \text{CD} = A(\Delta\theta \cdot defocus) + B(1 - \sqrt{1 - \Delta T}), \qquad (1)$$

where $\Delta\theta$ is the phase error and $\Delta T$ is the intensity transmission error. The phase error defines the slope of the $\Delta$CD curve. The $A$ and $B$ parameters in Equation (1) depend on the design of the alternating pattern and exposure system NA, wavelength, and partial coherence.

AIMS measurements were used to characterize an actual alternating PSM process. With the AIMS tool configured with $\lambda$ = 248 nm, NA = 0.5, and $\sigma$ = 0.6, aerial image measurements were taken through focus for a 0.20-$\mu$m alternating line/space grating, as shown in **Figure 10.** The difference in intensity peak width for lines of opposite phase was determined as a function of focus and plotted in **Figure 11** at multiple thresholds. A value of phase was then

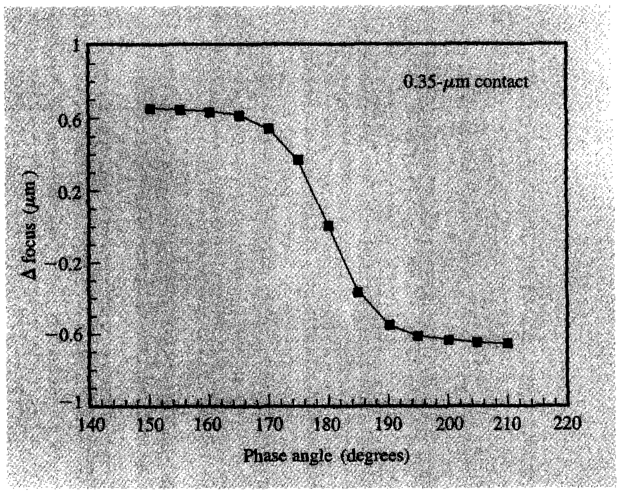


**Figure 13**

Relationship between attenuated mask phase angle relationship and focus offsets. (Reprinted with permission from [5]).

extracted using Equation (1). The phase was found to be 5° from optimum, requiring an etch depth correction.

Effects of the phase error observed in the AIMS measurements were also confirmed using stepper exposures on the Micrascan® II from SVG Lithography Systems, Inc. (SVGL). **Figures 12(a)** and **12(b)** respectively show the 0.20-μm pattern in 0.6 μm of APEX-E resist at 0 and 0.25-μm defocus. The defocused condition clearly shows resist openings of differing width, in contrast to the 0.0 defocus condition, in which all resist openings are of uniform width. This is consistent with the aerial image, in which neighboring intensity peaks vary in size for the defocused condition.

The phase of an attenuating PSM is particularly difficult to ascertain, since it depends on the real and imaginary parts of the refractive index of the phase-shifting material as well as the depth into the mask substrate. The AIMS tool, however, provides a means of measuring the phase through the comparison of aerial image focus characteristics of a contact and lines [9, 10]. Small contact holes receive the greatest improvement of all feature types from attenuating phase shifting, and are therefore the most sensitive to any phase error. The action of a phase error is to shift the optimal focal plane in either a positive or a negative direction. Other structures such as the line/space grating are not as sensitive to phase, producing a significantly smaller change to the feature's focus characteristics. By quantifying the difference in focus at which a maximum size is achieved for a contact and nested lines, the AIMS tool can be used to determine attenuated PSM phase errors. Fabrication parameters can then be optimized. **Figure 13** shows the difference in focus for a 0.35-μm contact compared to a 0.35-μm line/space pattern as a function of phase error.

The ability of the AIMS tool to identify fabrication errors rapidly makes it ideal for mask qualification, in which good reticles can be separated from bad. This is

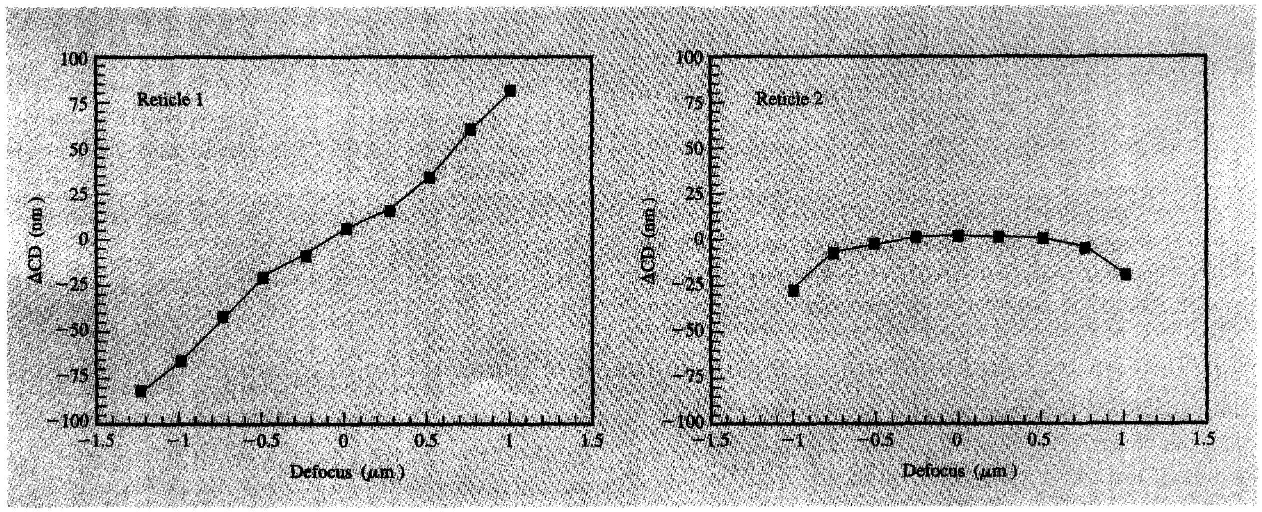


**Figure 14**

AIMS measurements of ΔCD through-focus from two reticles with alternating PSM DRAM cell pattern of Figure 8. (Reprinted with permission from [5]).

demonstrated with the DRAM cell feature in Figure 8. Two masks were fabricated with this pattern using the same manufacturing process. **Figure 14** shows the ΔCD versus defocus characteristics of the two reticles. A significantly larger phase error exists for the first reticle, as exhibited by the large slope of the ΔCD curve versus the near-zero slope of the second reticle. This conclusion was further supported with exposure-defocus analysis, which showed a 62% improvement in DOF for a 15% variation in exposure for the second reticle compared to the first. In addition, the improved performance was confirmed using stepper exposures on the SVGL Micrascan II.

Lithographic performance optimization is required once fabrication parameters are established and mask qualification is complete. The AIMS tool provides a rapid means of optimization for stepper parameters such as numerical aperture and partial coherence [11]. This is demonstrated for the 0.20-$\mu$m alternating line/space grating shown in Figure 10. Aerial image measurements were taken through focus with the AIMS configured at $\lambda = 248$ nm, NA = 0.5, and $\sigma = 0.6$ and 0.3. **Figure 15** shows the intensity distributions, with the 0.3 partial coherence clearly having improved image contrast and through-focus performance. Quantification of the improvement is established through an exposure-defocus analysis.

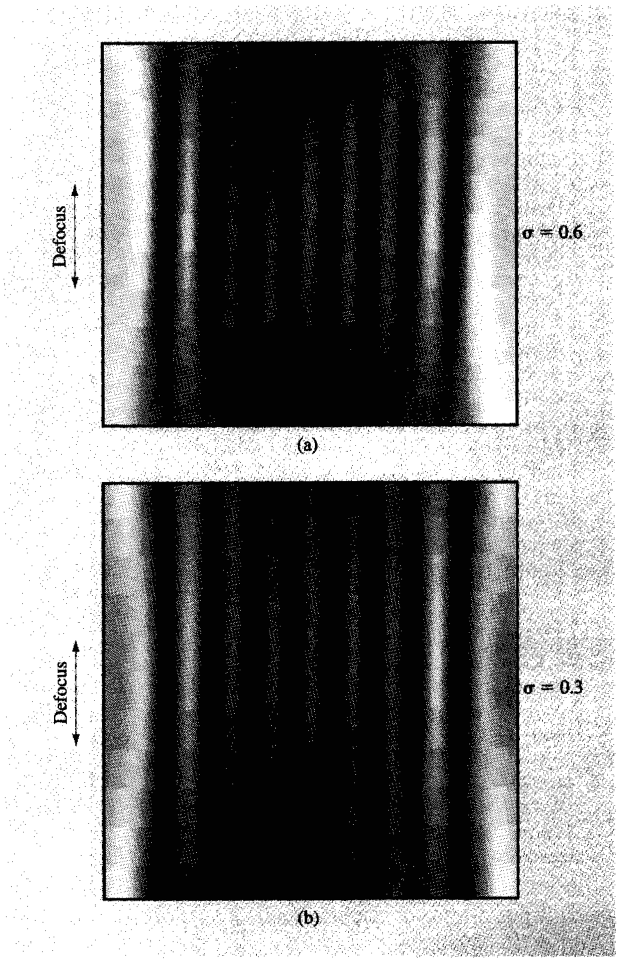


**Figure 15**

Intensity distribution through-focus, 0.2-$\mu$m line/space pattern, $\lambda = 248$ nm, NA = 0.5: (a) $\sigma = 0.6$; (b) $\sigma = 0.3$.

## Summary

The Aerial Image Measurement System has been introduced for evaluating lithographic masks; its application to the development of advanced mask designs has been described, and details of its optical system and its software capability have been given. It has been found that analysis of the stepper equivalent image produced by the AIMS tool provides a new capability for rapid evaluation of the printing properties of chrome and phase-shifted masks prior to undertaking extensive resist-validation exposures and SEM feature size measurements. Examples have been presented demonstrating its application to the optimization of the mask fabrication process, measurement of mask phase error, characterization of feature printability, and optimization of mask photolithographic performance.

## Acknowledgments

The authors wish to thank Omesh Sahni for his continuing support and encouragement, as well as colleagues at IBM and Carl Zeiss Inc. for many useful interactions.



## References

1. M. D. Levenson, N. Viswanathan, and R. Simpson, "Improving Resolution in Photolithography with a Phase-Shifting Mask," *IEEE Trans. Electron Devices* **ED-29,** 1828–1836 (1982).
2. B. J. Lin, "The Optimal Numerical Aperture for Attenuated Phase-Shifting Masks," *Microelectron. Eng.* **17,** 79–86 (1992).
3. R. A. Budd, J. Staples, and D. B. Dove, "A New Tool for Phase Shift Mask Evaluation, the Stepper Equivalent Aerial Image Measurement System AIMS," *Proc. SPIE* **2087,** 162–171 (September 1993).
4. R. A. Budd, D. B. Dove, J. L. Staples, H. Nasse, and W. Ulrich, "A New Mask Evaluation Tool, the Microlithography

Simulation Microscope Aerial Image Measurement System," *Proc. SPIE* **2197,** 530–540 (March 1994).

5. R. A. Ferguson, R. M. Martino, R. A. Budd, J. Staples, L. W. Liebmann, D. B. Dove, and J. T. Weed, "Application of an Aerial Image Measurement System to Mask Fabrication and Analysis," *Proc. SPIE* **2087,** 131–144 (September 1993).
6. R. A. Ferguson, W. J. Adair, D. S. O'Grady, R. M. Martino, A. F. Molless, B. J. Grenon, A. K. Wong, L. W. Liebmann, A. C. Callegari, D. C. La Tulipe, D. M. Sprout, and C. M. Seguin, "Impact of Attenuated Mask Topography on Lithographic Performance," *Proc. SPIE* **2197,** 130–139 (March 1994).
7. U. Boettiger, T. Fischer, A. Grassmann, and H. Ritz, "Aerial Image Analysis of Quarter Micron Patterns on a 0.5 NA Excimer Stepper," *Proc. SPIE* **2197,** 402–411 (March 1994).
8. A. K. Wong, R. A. Ferguson, and A. R. Neureuther, "Phase Shifter Edge Effects on Attenuated Phase Shifting Mask Image Quality," *Proc. SPIE* **2197,** 122–129 (March 1994).
9. R. Martino, R. Ferguson, R. Budd, J. Staples, L. Liebmann, A. Molless, D. Dove, and J. Weed, "Application of the Aerial Image Measurement System (AIMS) to the Analysis of Binary Mask Imaging and Resolution Enhancement Techniques," *Proc. SPIE* **2197,** 573–584 (March 1994).
10. A. K. Wong, R. A. Ferguson, R. M. Martino, and A. R. Neureuther, "Focus Shift and Process Latitude of Contact Holes on Attenuated Phase Shifting Masks," *Proc. SPIE* **2440,** 472–479 (February 1995).
11. L. W. Liebmann, T. H. Newman, R. A. Ferguson, R. M. Martino, A. F. Molless, M. O. Neisser, and J. T. Weed, "A Comprehensive Evaluation of Major Phase Shift Mask Technologies for Isolated Gate Structures in Logic Designs," *Proc. SPIE* **2197,** 612–623 (March 1994).

*Received February 9, 1996; accepted for publication October 15, 1996*

**Russell A. Budd** *IBM Research Division, Thomas J. Watson Research Center, P.O. Box 218, Yorktown Heights, New York 10598 (rbudd@watson.ibm.com).* Mr. Budd is a senior engineer in the Subsystem Technical and Applications Laboratory at the Thomas J. Watson Research Center. In 1977 he received a B.S. degree from Michigan State University in mechanical engineering; he joined IBM at Boulder, Colorado, that same year. His work while at IBM Boulder involved the design of photocopier and laser printer optical systems. Since joining the Thomas J. Watson Research Center, Mr. Budd has helped to develop the AIMS system; he now works on miniature displays. He is a member of the Optical Society of America and the American Society of Mechanical Engineers.

**Derek B. Dove** *IBM Research Division, Thomas J. Watson Research Center, P.O. Box 218, Yorktown Heights, New York 10598 (dove@watson.ibm.com).* Dr. Dove attended the Imperial College of Science and Technology, London, England, receiving the Ph.D. degree in 1956. After working at AERE, Harwell, for several years, he joined Bell Telephone Laboratories, Murray Hill, New Jersey, where he was involved in studies on the structure and properties of magnetic films. In 1967 he became professor of Materials Science and Electrical Engineering at the University of Florida. In 1977, Dr. Dove joined IBM at Yorktown Heights as a manager in the display and printing area, where he worked on resistive ribbon printing and on electrophotography. More recently, he has worked on phase-shift masks and on optical systems for high-resolution displays.

**John L. Staples** *IBM Research Division, Thomas J. Watson Research Center, P.O. Box 218, Yorktown Heights, New York 10598 (staples@watson.ibm.com).* Mr. Staples received the B.S. degree in electrical engineering from Fairleigh Dickinson University. Since joining the IBM Thomas J. Watson Research Laboratory, he has worked on a variety of research projects in applied physics, electronics, and optics, including characterization of high-frequency transistors, Gunn-effect microwave devices, plasma display devices, multibeam high-resolution CRT displays, high-resolution laser printers, rf data entry devices, rf and EMI detection and suppression, and the Aerial Image Measurement System. Mr. Staples is currently involved in the development of high-resolution liquid-crystal color display systems. He holds several U.S. and foreign patents and has authored several papers and patent publications.

**Ronald M. Martino** *IBM Microelectronics Division, East Fishkill facility, Hopewell Junction, New York 12533 (rmartino@vnet.ibm.com).* Mr. Martino received his B.S. degree in chemical engineering from Drexel University in 1988, and his M.S. degree in materials science in 1991 from the University of Vermont. He joined IBM in 1988 and has held several engineering positions in mask and semiconductor development. He currently works at the Semiconductor Research and Development Center in East Fishkill, New York, in advanced lithography development for product applications in DRAM memory and logic. Mr. Martino is manager of Design Rules, Manufacturing Aids, and Test Sites for advanced logic technologies in the IBM Microelectronics Division.

**Richard A. Ferguson** *IBM Microelectronics Division, East Fishkill facility, Hopewell Junction, New York 12533 (rich_ferguson@vnet.ibm.com).* Dr. Ferguson received his B.S. degree in electrical engineering from Duke University in 1985. He received his M.S. in 1987 and his Ph.D. in 1991 from the University of California at Berkeley, where he worked on the modeling and simulation of advanced resist processes for optical lithography. Since 1991, Dr. Ferguson has been working at the IBM Semiconductor Research and Development Center in East Fishkill, New York, in advanced lithography development for product applications in DRAM memory and logic.

**J. Tracy Weed** *IBM Microelectronics Division, East Fishkill facility, Hopewell Junction, New York 12533 (tweed@fshvm1.vnet.ibm.com).* Dr. Weed received his B.S. and M.S. degrees in structural inorganic chemistry from the University of Connecticut. He received his Ph.D. in 1984 from the University of California at Riverside in the area of synthetic organometallic chemistry. Dr. Weed joined IBM in 1984 and has held several engineering and management positions in packaging and semiconductor development. Most recently he was manager of the advanced lithography applications group at the IBM Semiconductor Research and Development Center. He is currently program manager of Semiconductor Manufacturing Strategy for the IBM Microelectronics Division.